Research Paper

Thermal simulation of a social dwelling in Chile: Effect of the thermal zone and the temperature-dependant thermophysical properties of light envelope materials

Diego A. Vasco [a,*], Manuel Muñoz-Mejías [a], Rodrigo Pino-Sepúlveda [a], Roberto Ortega-Aguilera [a], Claudio García-Herrera [b]

[a] Departamento de Ingeniería Mecánica, Universidad de Santiago de Chile, Av. Lib. Bernardo O'Higgins 3363, Santiago, Chile
[b] Facultad de Ingeniería y Ciencias, Universidad Adolfo Ibáñez, Av. Diagonal las Torres 2640, Peñalolén, 7941169, Santiago, Chile

HIGHLIGHTS

- Temperature-dependent thermal properties of building materials were measured.
- Thermal conductivity of EPS is more sensitive to temperature variation.
- The envelope of a social dwelling in each thermal zone from Chile was simulated.
- In Southern Zones, thermal regulated envelopes help to maintain comfort.
- In Northern Zones, thermal regulated envelopes fail to maintain thermal comfort.

ARTICLE INFO

ABSTRACT

As in most countries, Chile exhibits a continuous growth of energy demand, although nowadays the country does not have enough conventional energy sources to supply it. For this reason, energy saving approaches in the residential sector have been encouraged. One of the solutions to improve the energy performance of the buildings is to decrease wasting energy through the building's envelope, therefore the thermal properties of materials used in building envelopes must be analyzed to evaluate the thermal response of houses. Normally, the thermal envelope of a social house in Chile is made of brick or wood along with light materials such as fiber cement, plasterboard, and thermal insulating materials as polystyrene foam. The experimental part of this work deals with the measurement of the thermal conductivity and thermal diffusivity of the aforementioned light materials in a temperature range from $-5\,°C$ to $40\,°C$ through the transient line heat source method. The experimental results allowed the identification of 10–20% variation of those thermophysical properties. The response of the thermal envelope and the inner temperature of a social dwelling under seven different climatological conditions was evaluated through transient simulations with EnergyPlus. The results allowed to identify that the dwellings located in hotter zones are prone to having higher temperatures than the comfort temperature, and the recommendations of the thermal regulations in Chile are more effective in the colder thermal zones 6 and 7.

© 2016 Elsevier Ltd. All rights reserved.

1. Introduction

Most of the existing buildings are responsible for an important share of the overall energy consumption, and they generate a large proportion of the greenhouse effect in the world. In developed countries the buildings contribution to total energy consumption is between 20% and 40% [1]. In Europe, buildings, commercial and residential, account for 38.7% of the total energy consumption [2], and in US commercial buildings alone expend approximately 18% of the total energy consumption [3]. Buildings generate a large proportion of the greenhouse gas in the world, and that it is why the International Energy Agency has claimed that the building sector must reduce its total CO_2 emissions by 60% in 2050 to limit global temperature rise to $2\,°C$ [4].

In Chile during the last decade the consumption of electrical energy in the residential sector has shared 16% of the demand electrical energy [5]. The average consumption of energy, including all

* Corresponding author.
  E-mail address: diego.vascoc@usach.cl (D.A. Vasco).

Nomenclature

U	conductive thermal transmittance	h_c	convective coefficient for smooth surfaces
C_z	product of the density and specific heat of air	h_n	natural convective coefficient
N_{sl}	number of convective internal loads	$h_{c,r}$	convective coefficient for roughened surfaces
N_{surf}	number of zone surfaces	R_f	dimensionless factor which accounts for the roughness of the surface
N_{zones}	number of zones		
$\dot{Q}_i$	convective thermal load i	V_z	wind velocity
h_i	convective heat transfer coefficient in zone i	V_{met}	average meteorological wind velocity
A_i	area of surface i	a, b	constants that depend on wind direction
T_{si}	temperature of surface i	ΔT	temperature difference
T_{zi}	temperature of zone i	σ	inclination angle of the surface
$\dot{m}_i$	mass flow due to interzone air mixing	z	altitude, height above ground
$\dot{m}_{inf}$	mass flow due to infiltration of outside air	α	wind speed profile exponent at the site
T_∞	ambient temperature	δ	wind speed profile boundary layer thickness at the site
T_z^t	temperature of zone at present time step	z_{met}	height above ground of the measuring device at the meteorological station
T_z^{old}	temperature of zone at a previous time step		
δt	envelope time discretization	α_{met}	wind speed measured at the meteorological station
k_E	thermal conductivity of the east node	δ_{met}	wind speed profile boundary layer thickness at the meteorological station
k_W	thermal conductivity of the west node		
Δx	spatial discretization	k	thermal conductivity
Δt	zone time discretization	C_p	specific heat capacity
Fo	Fourier number ($\alpha \Delta t / \Delta x^2$)	ρ	density
$\dot{Q}_{sys}$	air systems output	T	temperature

sources, of a house in Chile is 10,232 kW h/year. This value is considered high and it can be explained by the share of the use of wood as an energy source (46.6%) in the south of the country, mainly due to its lower price and availability in comparison with other sources. In southern Chile, wood is used mainly to maintain thermal comfort conditions in houses [6].

One of the main solutions to improve the energy performance of a building is to manage the heat flow through its thermal envelope. Most energy used in the residential sector is mainly for space heating and cooling, and therefore, to reduce energy consumption energy-smart house wall systems are required [7]. A high performance building envelope is one of the prerequisites and foundation of a zero energy building (ZEB). Near ZEB is a high energy performance building that requires a very small amount of energy, and its energy needs are covered by energy coming from renewable sources [8]. A building envelope includes mainly the transparent and non-transparent one, also called as opaque envelope, which it is in contact with the outside environment; they can also be further classified into external envelopes and internal envelopes [9]. Two main functions that envelopes must fulfill from the energy-saving perspective are (i) preventing heat loss from the indoor environment, and (ii) managing solar gain. Regarding the first function, the main property of the building envelope to look at is the thermal insulation capability, usually expressed by the thermal transmittance. With respect to the solar gain, the main property of the building envelope to be concern about is thermal inertia [10].

Traditional analytical methods are not useful when temperature dependent thermophysical properties and variable weather conditions are considered. Among all ASHRAE cooling load methods, the heat balance method is recognized as the most rigorous and accurate method that establishes the energy balance equations for a building, based on the first principle of thermodynamic [11]. Therefore, an alternative to analyze temperature variation and energy consumption in buildings is to use a supported computational tool such as EnergyPlus. The numerical predictions of this open-source software have been validated with experimental measurements in several related studies [12–15]. EnergyPlus has

even been used to validate a proposed model, which describes the inner radiation effect on the external envelopes of a building [16]. However, the importance of making an adequate refinement of space and time, to obtain realistic numerical predictions, has been pointed out [17,18]. Merely computational studies have been performed. Obyn and Moeseke [19] evaluated the effect of convective heat transfer coefficient models on heating and cooling demands and maximal loads in a standard office building by using TRNSYS 17. The authors analyzed several types of envelope, orientation and internal gains levels to evaluate the impact of the convective models. Nan et al. [20] carried out the calculation of energy demand in a domestic dwelling considering details such as occupancy pattern, lighting and appliance schedule through the ESP-r building simulation software.

Thermal properties of materials used in building envelopes must be analyzed in order to evaluate the thermal response of the construction system. This thermal characterization is a key point during the design phase of the building. It is important to test materials that will be used in the construction of building envelopes before implementing them [21]. The present work is focused first on the thermal characterization of the materials of the thermal envelope. Especially, the thermal properties of the lighter materials are studied as a function of temperature (−5 °C to 40 °C). The second part of the paper deals with the transient simulation with EnergyPlus of a social dwelling that complies with the Chilean thermal regulations, located in the thermal zones into which the country is divided. The results are presented for each thermal zone as transient temperature during a week of each season and the transient temperature distribution along a wall of the thermal envelope during a chosen day of the seasons.

2. Thermal regulation of dwellings in Chile

Due to its geographical position with respect to high pressure zones, the presence of a polar front and the influence of the Pacific Ocean and the Andes mountains, Chile has a variety of climates. The elevation of the western coast mountains do not allow the flow

of the sea winds and the Andes mountains inhibit the influence of the continental climate. The long coast and the Humboldt current turn the country's climate in predominantly marine, which moderates temperature through the development of clouds and fresh winds. Humidity, rains, lower temperatures, and winds are more distinctive characteristics of southern Chile, while the north of the country is dryer, with a desert climate. In 2006 the Ministry of Housing and Urban Development of Chile set down act 192, which establishes that *all housing must meet the requirements of thermal conditioning* specified in Tables 1 and 2. The thermal zoning of Chile is based on the heating degree-days (HDD) concept, which in a specified period of time (winter), is obtained as the summation of the differences between a base temperature (15 °C) and the day-averaged temperatures minus the base temperature. The heat to overcome the difference between the base temperature and the comfort temperature is supplied by the internal heat gains such as occupants, appliances, and lighting. According to this, the act has established the conductive thermal transmittance (U) of the envelope of dwellings for each thermal zone of Chile. Table 1 specifies the cities where the weather data is available and where thermal simulations are performed. The weather data were acquired from White Box Technologies. The act does not mention the temperature at which the thermal resistance should be calculated, which is important since the thermophysical properties of building materials may vary significantly with temperature. Moreover, it is worth mentioning that the availability of thermal properties of building materials is limited to constant or narrow temperature ranges [22].

3. Experimental determination of thermophysical properties of the building materials

The samples used during the measurements were taken from commercially available materials. The size of the samples were prepared keeping their manufacturing thickness: fiber cement board (6 mm), plasterboard (10 mm), and polystyrene foam (50 mm). The thermal conductivity and volumetric heat capacity are two thermophysical properties which can strongly influence the energy performance of the envelope [9]. The measurement of the properties has been performed by the transient line heat source method (*KD2-Pro, Decagon devices*). The probe for this measurement consists of a needle with a heater and a sensor inside. A current is passed through the heater and the temperature of the probe is monitored over time. In the present work two kind of needles were used. The dual needle probe (*sh1*), which was used in the determination of the thermal properties (thermal conductivity and thermal diffusivity) of fiber cement board (*FC*) and plasterboard (*PB*), and the single needle probe (*ks-1*), which was used for the determination of thermal conductivity of polystyrene foam (*EPS*). The measurements were made in triplicate over temperature from −5 °C to 40 °C. Temperatures between 20 °C and 40 °C were measured in an oven (*Hareus*) with a precision of ±0.1 °C. For the

lower temperature range, from −5 °C to 15 °C, a temperature-controlled (*Danfoss*) mechanical-compression refrigeration system with a precision of ±0.1 °C, was built. Both the oven and the refrigeration system were used as controlled temperature environments. The temperatures are really measured by the probes of KD2-Pro. The experimental setup is illustrated in Fig. 1.

The density of the building materials was determined by weighing a known volume of the samples with an analytical balance (*Bel Engineering*, ±0.01 g). The volumes of *PB* and *EPS* were determined by measuring the lengths of square-prism shaped samples with a calliper (*Mitutoyo*, ±0.01 mm). The volume of the sample of *ACB* was obtained by the displacement method (test tube, ±0.5 mm³). According to these measurements the obtained bulk densities are shown in Table 3. Volume and mass measurements were made in triplicate, therefore densities in Table 3 are average values. The obtained thermal conductivity and thermal diffusivity as a function of temperature of *FC*, *PB*, and *EPS* are shown in Figs. 2 and 3, respectively. The thermal conductivity of *ACB* increases with temperature 0.0004 W/mK per 1 °C, while thermal diffusivity decreases approximately 0.0002 mm²/s per 1 °C. In the case of *PB*, its thermal conductivity exhibits a less sensitive variation with temperature (0.0002 W/mK per 1 °C) and the variation of thermal diffusivity with temperature is quite similar to that observed with *FC* (0.00025 mm²/s per 1 °C). EPS thermal conductivity is more sensitive to temperature variation. In the temperature range from −5 °C to 20 °C, thermal conductivity increases 0.02 W/mK per 1 °C, at higher temperatures the thermal conductivity tends to be almost constant. Due to its low thermal diffusivity, the use of *KD2-Pro* with the dual needle probe *sh1* is not advisable. Therefore, for the subsequent studies a constant value for specific heat capacity of 1210 J/kgK is assumed [23].

The behavior of volumetric heat capacity as a function of temperature of *FC* and *PB* is shown in Fig. 3. It can be seen how both properties increase with temperature in the analzed temperature range. Volumetric heat capacity of *ACB* and *PB* increases 0.0021 MJ/m³ K per 1 °C and 0.0024 MJ/m³ K per 1 °C, respectively. These thermophysical properties in the specified temperature range are used in the computational simulation of the dwellings located in the different thermal zones of Chile.

Table 2
Maximum percentage area of glazed surfaces based on the height of the walls.

Thermal zone	Monolithic glass	Hermetic double glazed units	
		3.6 ⩾ U [W/m² K] > 2.4	U [W/m² K] > 2.4
1	50	60	80
2	40	60	80
3	25	60	80
4	21	60	75
5	18	51	70
6	14	37	55
7	12	28	37

Table 1
Thermal transmittance (U) for each thermal zone in Chile according to the concept of heating degree-days (HDD).

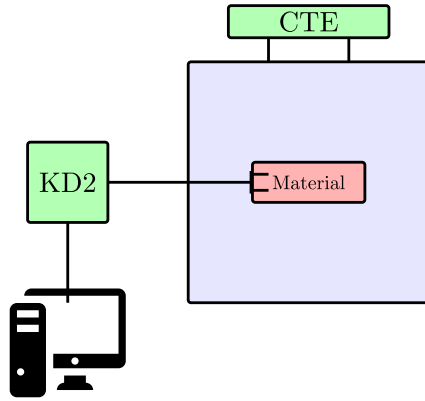| Thermal zone	Heating degree-days	U [W/m² K]			Cities
zone	degree-days	Walls	Roof	Vent. floor	(locality)
1	⩽500	4.0	0.84	3.60	Antofagasta
2	>500–⩽750	3.0	0.60	0.86	Viña del Mar
3	>750–⩽1000	1.9	0.47	0.70	Santiago (Puente Alto)
4	>1000–⩽1250	1.7	0.38	0.60	Concepción
5	>1250–⩽1500	1.6	0.33	0.50	Temuco
6	>1500–⩽2000	1.1	0.28	0.39	Puerto Montt
7	⩾2000	0.6	0.25	0.32	Punta Arenas

Fig. 1. Experimental setup for thermal properties measurement in a controlled temperature environment (CTE).

Table 3
Experimental bulk densities of the building materials.

Building material	Bulk density, $\bar{\rho}$ [kg/m³]	Density [22], [kg/m³]
Fiber cement board	1200.87 ± 13.39	1900
Plasterboard	718.48 ± 4.58	640
Polystyrene foam	9.36 ± 0.06	16–24

4. Simulation tool and numerical formulation

The computational analysis proposed in this paper is based on building computational simulations using EnergyPlus, which is a well-recognized and accepted building energy analysis software tool [24,25]. EnergyPlus has been used by engineers, architects and researchers to model both energy consumption (heating, cooling, ventilation) and water use in buildings. To obtain the transient temperature values within a zone, EnergyPlus implements an energy balance Eq. (1) for each room of a dwelling. The left side term of the equation is the thermal energy store in zone air, which contains the term C_z that it is the product of the density and specific heat of air. The right side terms of the equation corresponds to: (i) sum of the convective internal loads, (ii) convective heat transfer from the zone surfaces, (iii) heat transfer due to infiltration of outside air, (iv) heat transfer due to inter-zone air mixing, (v) air systems output, respectively.

$$C_z \frac{dT_z}{dt} = \sum_{i=1}^{N_{sl}} \dot{Q}_i + \sum_{i=1}^{N_{surf}} h_i A_i (T_{si} + T_z) + \sum_{i=1}^{N_{zones}} \dot{m}_i C_p (T_{zi} + T_z)$$
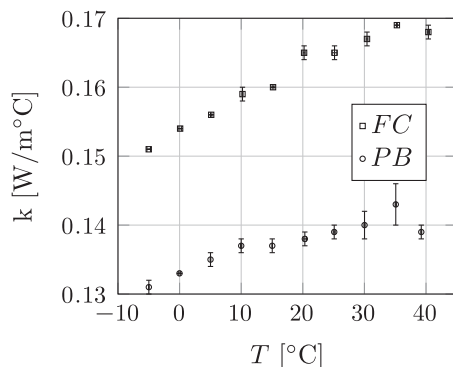$$+ \dot{m}_{inf} C_p (T_\infty + T_z) + \dot{Q}_{sys} \tag{1}$$

The main goal of this work is to evaluate only the performance of the thermal envelope of the social dwelling under different weather conditions in Chile, therefore no internal loads, air mixing, HVAC equipment and infiltrations were taking into account, and only the convective heat transfer term (ii) in Eq. (1) is considered:

$$C_z \frac{dT_z}{dt} = \sum_{i=1}^{N_{surf}} h_i A_i (T_{si} + T_z) \tag{2}$$

EnergyPlus implements by default the third order backward finite difference approach to solve (2), giving place to higher-order truncation errors and allowing for the use of larger time steps in the simulation. The zone temperature equation becomes:

$$T_z^t \left(\frac{11}{6} \frac{C_z}{\delta t} + \sum_{i=1}^{N_{surf}} h_i A_i \right) = \sum_{i=1}^{N_{surf}} h_i A_i T_{si} - f(T_z^{old}) \tag{3}$$

where:

$$f(T_z^{old}) = \frac{C_z}{\delta t} \left(-3T_z^{t-\delta t} + \frac{3}{2} T_z^{t-2\delta t} - \frac{1}{3} T_z^{t-3\delta t} \right) \tag{4}$$

For the calculation of the transient variation of temperature in the thermal envelope of a building, EnergyPlus implements a finite difference discretized version of the conduction transfer equation. The software includes two options for the formulation of the transient term: the semi-implicit Crank-Nicholson formulation and the fully implicit formulation. The implemented Crank-Nicholson scheme, which it is second-order in time, is given by (5):

$$C_p \rho \Delta x \frac{T_i^{j+1} - T_i^j}{\Delta t} = \frac{1}{2}$$
$$\times \left(k_W \frac{T_{i+1}^{j+1} - T_i^{j+1}}{\Delta x} + k_E \frac{T_{i-1}^{j+1} - T_i^{j+1}}{\Delta x} + k_W \frac{T_{i+1}^j - T_i^j}{\Delta x} + k_E \frac{T_{i-1}^j - T_i^j}{\Delta x} \right)$$
$$\tag{5}$$

Since the chosen formulation is not fully implicit, the spatial discretization is restricted by the time discretization $\left(\Delta x = \sqrt{\frac{\alpha \Delta t}{Fo}} \right)$. The obtained system of algebraic equations is solved by the Gauss-Seidel method, and under-relaxation is used for increased stability.

5. Description of the dwelling

In each thermal zone of the country, the social dwelling under simulation corresponds to a house that fulfills the requirements of Chilean act 49, according to the built area (42–45 m²) and the requirements of the Chilean standards of urban planning and construction, according to minimum height of ceilings (2.3 m),
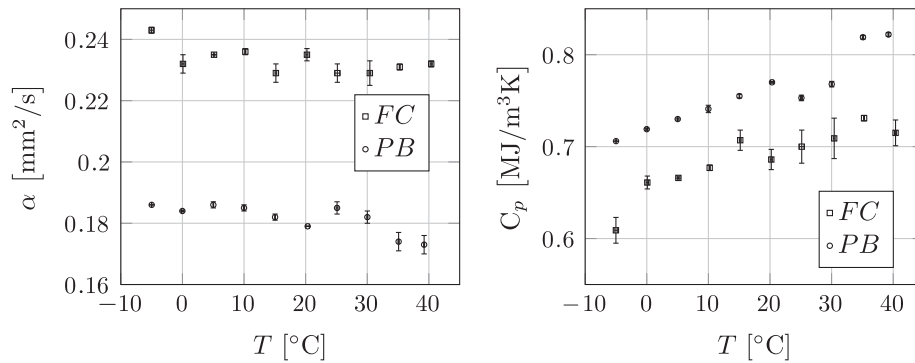

Fig. 2. Thermal conductivity of fiber cement board (*FC*), plasterboard (*PB*) and polystyrene foam (*EPS*).

Fig. 3. Thermal diffusivity and volumetric heat capacity of fiber cement board (*FC*) and plasterboard (*PB*).

number and position of windows, and thermal requirements of ceiling, walls and ventilated floors (Table 1) and windows (Table 2). For all simulations, the dwelling with six rooms has a built area of 44 m² and the façade faces the coordinate location of maximum incident solar radiation. As an example, the configuration of the house for thermal zone three is shown in Fig. 4.

According to the requirements of the Chilean standard for each thermal zone, modifications to the walls, floor and ceiling material thickness should be made. The wall configuration consists of four layers configured from the outside as fiber cement board (*FC*), brick, polystyrene foam (*EPS*), and plasterboard (*PB*). In the same way, the ceiling configuration consists of four layers configured as tile, *EPS*, pine wood, and *PB* and the floor is built by three layers of concrete, *EPS* and wood. The floor fulfill the settled thermal requirements for the walls. According to the thermal zone, the thickness of each layer is specified in Table 4. Wood and tile thickness were kept constant at 25 mm and 10 mm, respectively. It can be noticed as well how each configuration meets the requirements of the Chilean standard (Table 1). It should mentioned here that the

thermal properties of the building materials, brick, tile, pine wood, and concrete were assumed to be constant, and they were obtained from the ASHRAE Handbook [22], except brick and tiles, whose thermophysical properties were measured at constant temperature (Table 5). The convective coefficients used for the calculation of the thermal transmittance for the outer environment (Table 4) were obtained using the DOE-2 model, based on the experimental measurements performed by Kleims and Yazdanian for roughened surfaces [26]. DOE-2 is based on the MoWiTT and BLAST models [27,28]. The convective coefficient for smooth surfaces is given by:

Table 5
Thermophysical properties of the another implemented building materials.

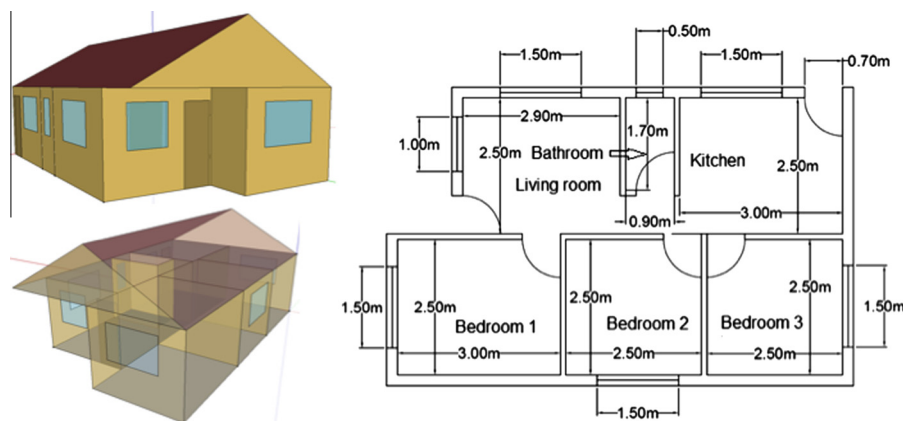| Building material	k [W/mK]	C_p [J/kg K]	ρ [kg/m³]
Brick	0.890	790	1920
Tile	0.890	790	1920
Pine wood	0.119	1636	447
Heavy concrete	1.95	900	2240

Fig. 4. Configuration of the simulated dwelling located in thermal zone three of Chile.

Table 4
Thickness (mm) of the building materials of the dwelling according to the thermal zone and the obtained transmittance coefficient (*U*).

Thermal zone	FC walls	Brick walls	PB Walls	PB Ceiling	EPS Walls	EPS Ceiling	h_{out} [W/m² K]	U [W/m² K] Walls	U [W/m² K] Ceiling
1	3	50	3	3	–	30	21.09	3.97	0.79
2	6	100	8	8	–	50	25.46	2.82	0.53
3	6	100	8	8	6	60	21.09	1.86	0.46
4	6	100	8	8	9	80	19.58	1.59	0.36
5	6	100	8	8	10	90	16.78	1.50	0.33
6	6	100	8	8	20	110	16.78	1.04	0.27
7	6	100	8	8	50	130	31.67	0.55	0.24

$$h_c = \sqrt{h_n^2 + (aV_z^b)^2} \qquad (6)$$

where h_n is the natural convection coefficient, V_z is the obtained wind velocity from the floor to the center of gravity of the surface, and a and b are constants that depend on the wind direction, respect to the surface. The coefficient h_n is obtained according to the sign of the temperature difference ΔT and the inclination angle of the surface σ:

$$h_n = \frac{9.482|\Delta T|^{1/3}}{7.283 - |\cos(\sigma)|} \qquad (7)$$

for $\Delta T < 0\,^\circ\mathrm{C}$ and surfaces facing upwards and $\Delta T > 0\,^\circ\mathrm{C}$ and surfaces facing downwards.

$$h_n = \frac{1.810|\Delta T|^{1/3}}{1.382 + |\cos(\sigma)|} \qquad (8)$$

for $\Delta T > 0\,^\circ\mathrm{C}$ and surfaces facing upwards and $\Delta T < 0\,^\circ\mathrm{C}$ and surfaces facing downwards.

Then, the convective coefficient for roughened surfaces is given by:

$$h_{c,r} = h_n + R_f(h_c - h_n) \qquad (9)$$

where R_f is a dimensionless factor which accounts for the roughness of the surface. The wind velocity V_z is obtained as a function of the average meteorological wind velocity (V_{met}) and the altitude of the measuring device in the weather station (z_{met}):

$$V_z = V_{met}\left(\frac{\delta_{met}}{z_{met}}\right)^{\alpha_{met}}\left(\frac{z}{\delta}\right)^{\alpha} \qquad (10)$$

where the values of $\alpha, \delta, \alpha_{met}$ and δ_{met} depend on the roughness characteristics of the surroundings. The average meteorologi-
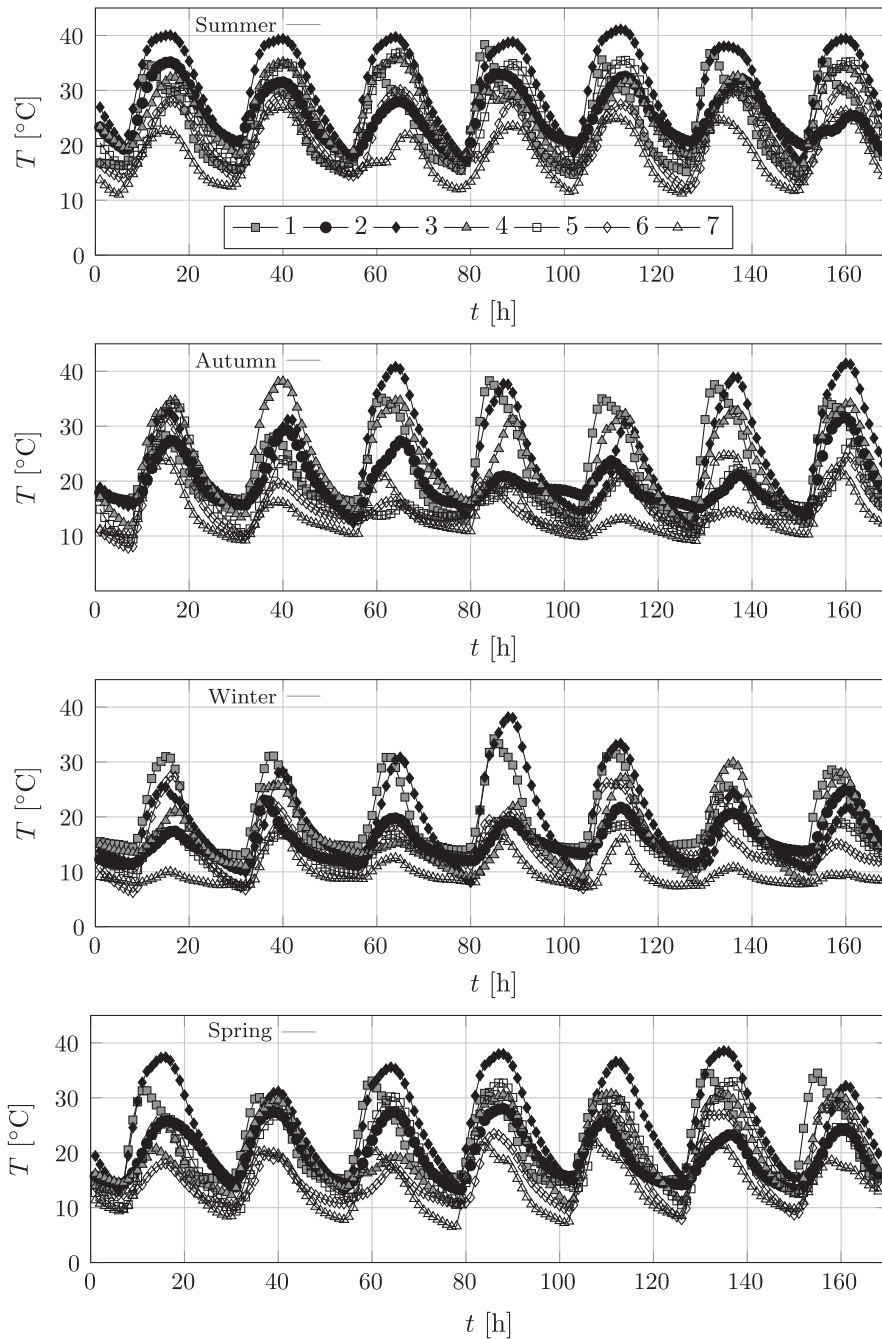

Fig. 5. Simulated temperature in the living-room of the dwelling during a season week for each thermal zone of Chile.

cal wind velocities were obtained from data provided by the Meteorological authority of Chile in 2014. A convective coefficient in the inner environment of 9.3 W/m² K was assumed as a constant for all thermal zones [22].

6. Results and discussion

6.1. Effect of thermal zone on temperature in the dwelling

Fig. 5 shows the distribution of temperature in the living-room of the dwelling during a seasonal week for each thermal zone. During summer, the higher temperatures are found in thermal zones 1, 3 and 5, reaching temperatures higher than 35 °C, while the lower temperatures are found in thermal zones 4 and 6, approximately 15 °C. During autumn there is a greater variation of temperature

between days. For instance, in thermal zones 1–4 the temperature can be as high as 40 °C and lower than 15 °C. In thermal zones 5, 6 and 7, temperatures are lower, ranging between almost 8 °C and 34 °C. During this season, comfortable days are observed in thermal zones 2 (16–21 °C), 5 (15–26 °C) and 6 (15–27 °C).

Even during the winter in Chile, inner high temperatures can be observed in thermal zones 1 (31 °C), 3 (37 °C) and 5 (34 °C). However, very low temperatures (10 °C) are predicted during certain days in the living-room of the dwelling located in thermal zones 5, 6 and 7. During winter, some comfortable days are predicted in thermal zones 1 and 2 (15–25 °C). During the chosen spring week in thermal zones 1 and 3, the observed temperature in the house can be as high as 37 °C and as low as 15 °C. In thermal zone 3 the temperature range is lower (18–33 °C) than in the former zones, and there are some comfortable days. In thermal zones 4, 5 and 6, 7 the tem-
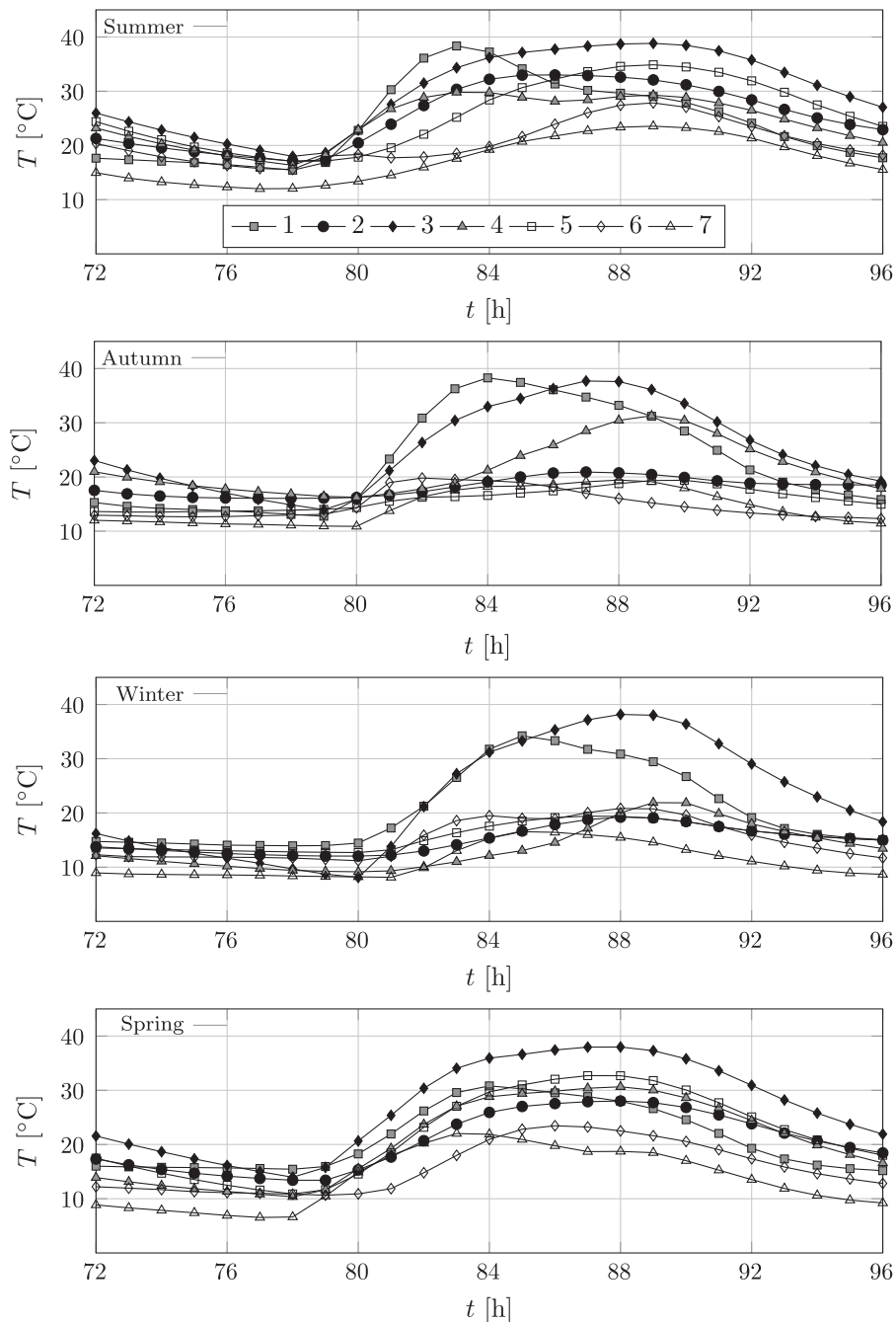

Fig. 6. Simulated temperature in the living-room of the dwelling during a season day for each thermal zone of Chile.

perature ranges are (10–30 °C) and (7–23 °C), respectively. During this season week, days of thermal comfort are not found.

A temperature distribution of the third day of the chosen season week is detailed in Fig. 6. In summer, the warmest periods are observed in the dwellings located in thermal zones 2, 3 and 5. In thermal zone 1, temperature rises steeply during the morning

and therefore a remarkable temperature peak occurs before mid-day. Temperature variation in the living room of the dwelling located in thermal zones 6 and 7 is not as high as in warmer zones, but in thermal zone 7 colder temperatures are predicted during morning hours. During autumn, the broader daytime temperature variations are found in the living room of the dwelling located in
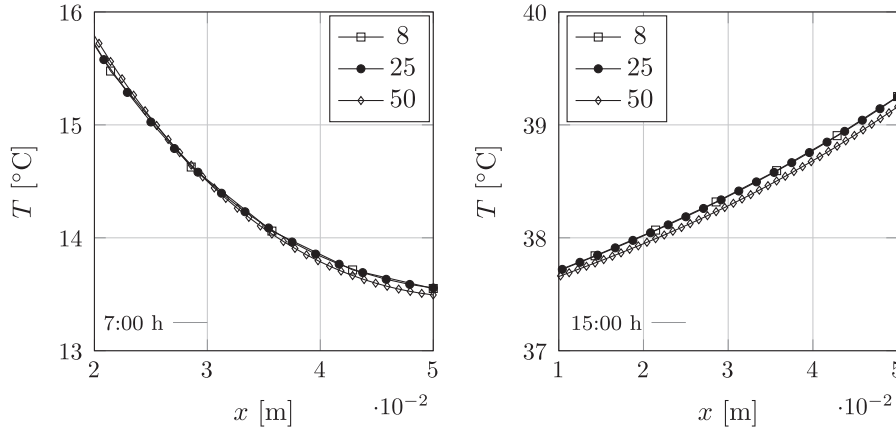

Fig. 7. Grid size independence analysis of the conduction problem in a thermal envelope configured as: *FC* (3 mm), *EPS* (10 mm), brick (50 mm) and *PB* (3 mm).
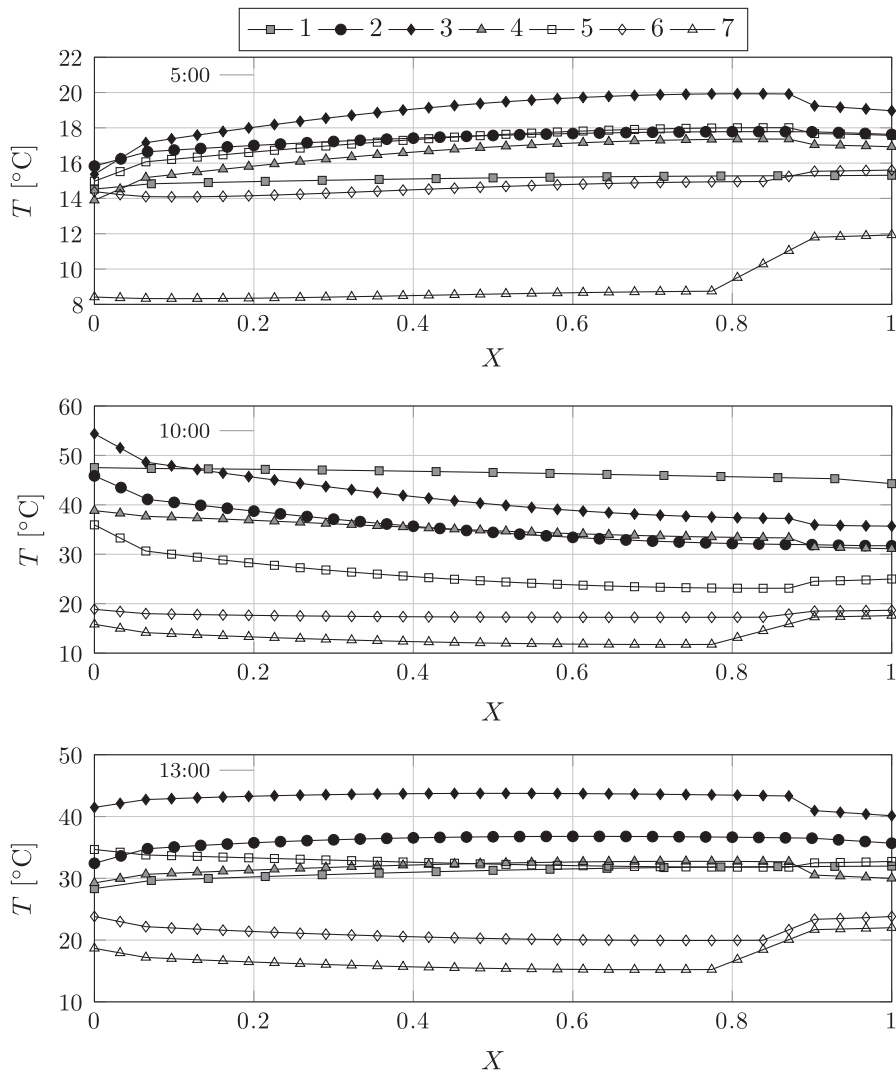

Fig. 8. Wall temperature distribution in the envelope during summer at different times.

thermal zones 1, 3 and 4. In the other thermal zones, temperature variations are lower and temperatures do not exceed 20 °C. In zone 6 the maximum temperature takes place before midday, meanwhile in thermal zones 5 and 7 the maximum temperature occurs after midday, around 14:00 h. In winter, the temperature variation is higher in the dwelling located in thermal zones 1 and 3. In the other thermal zones the temperature distribution is similar to that found during autumn in thermal zones 5 and 7. The effect of the colder season is more important in the temperature distribution of the dwelling located in thermal zone 4. Finally, during spring, it is seen that temperature variation is consecutively higher in thermal zones 3, 5, 4, 1 and 2, and actually excessively high in thermal zones 3 and 5. In thermal zones 6 and 7, comfortable temperatures are predicted in the afternoon (12:00–16:00 h), while the maximum temperature in thermal zone 7 occurs after midday, and in thermal zone 6 it takes place later.

6.2. Temperature profile in the thermal envelope

Prior to the study of the temperature distribution inside the walls of the thermal envelope, a grid size analysis was performed to show that the numerical results are independent of the domain discretization. The grid size independence analysis was carried out considering a cubic box with the following wall-configuration: FC

(3 mm), EPS (10 mm), brick (50 mm) and PB (3 mm). The temperature profile was obtained at two different times during the morning and afternoon of a summer day (Fig. 7). In Fig. 7 it is seen that the temperature profile is quite similar for the three studied grid sizes, but a slight temperature difference can be found between the results obtained from grid sizes of 25 and 50 nodes. Therefore for all zones, a grid of 32 nodes was considered fairly good to capture the heat conduction process, except in thermal zone 1 (15 nodes).

The temperature profile along the dimensionless thickness of a wall of the dwelling's thermal envelope is shown (Figs. 8–11). The analysis is performed considering three different times during a specific day of each season. Along with these results, outer (X = 0) and inner (X = 1) temperatures for each case are compiled in Tables 6 and 7, respectively. Generally, most of the inner temperatures are higher than the outer temperatures. Exceptions or quite close temperature values are highlighted in Table 6. In a dwelling, a comfortable temperature is considered between 18 °C and 20 °C during winter and autumn and between 23 °C and 25 °C during summer and spring [22]. The temperatures that fulfill those conditions are highlighted in Table 7.

Fig. 8 shows the corresponding temperature profiles at three times of a *summer* day (01/18). At 5:00 h, it is seen that the temperature distribution along the wall is fairly constant in thermal zone
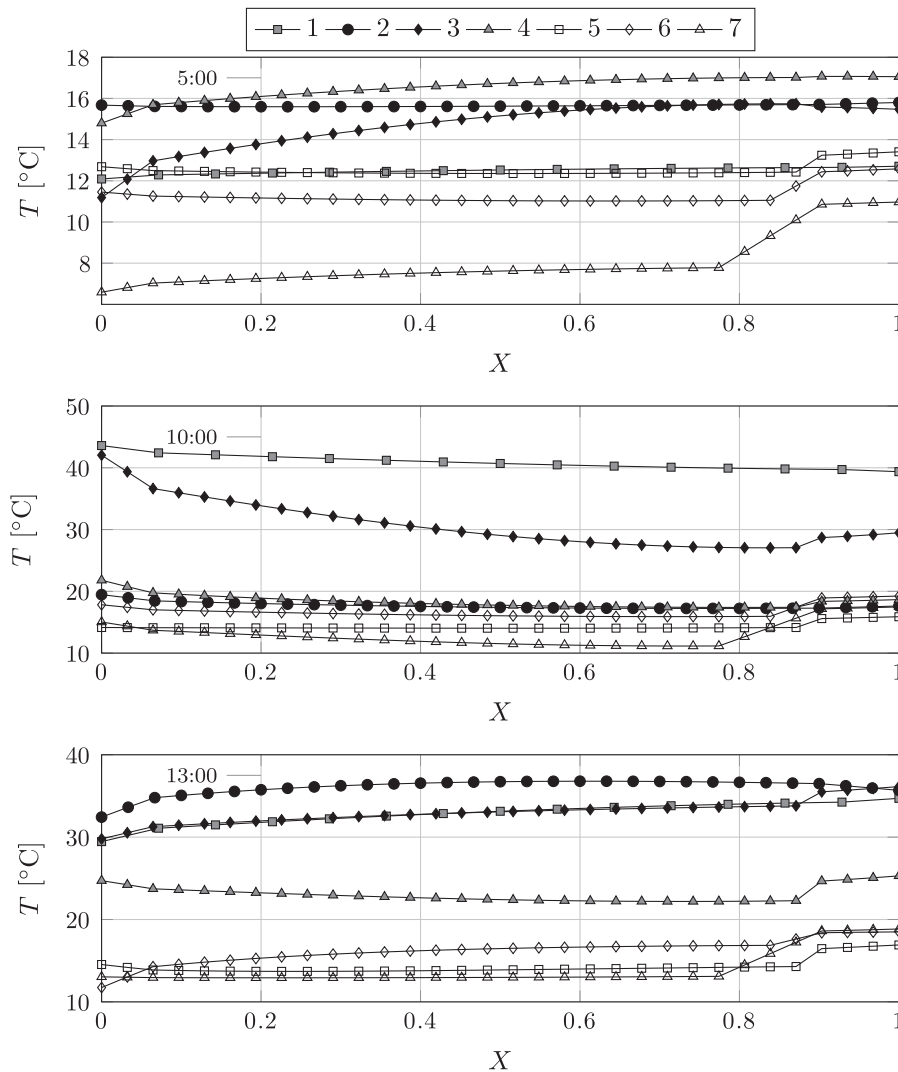

Fig. 9. Wall temperature distribution in the envelope during autumn at different times.
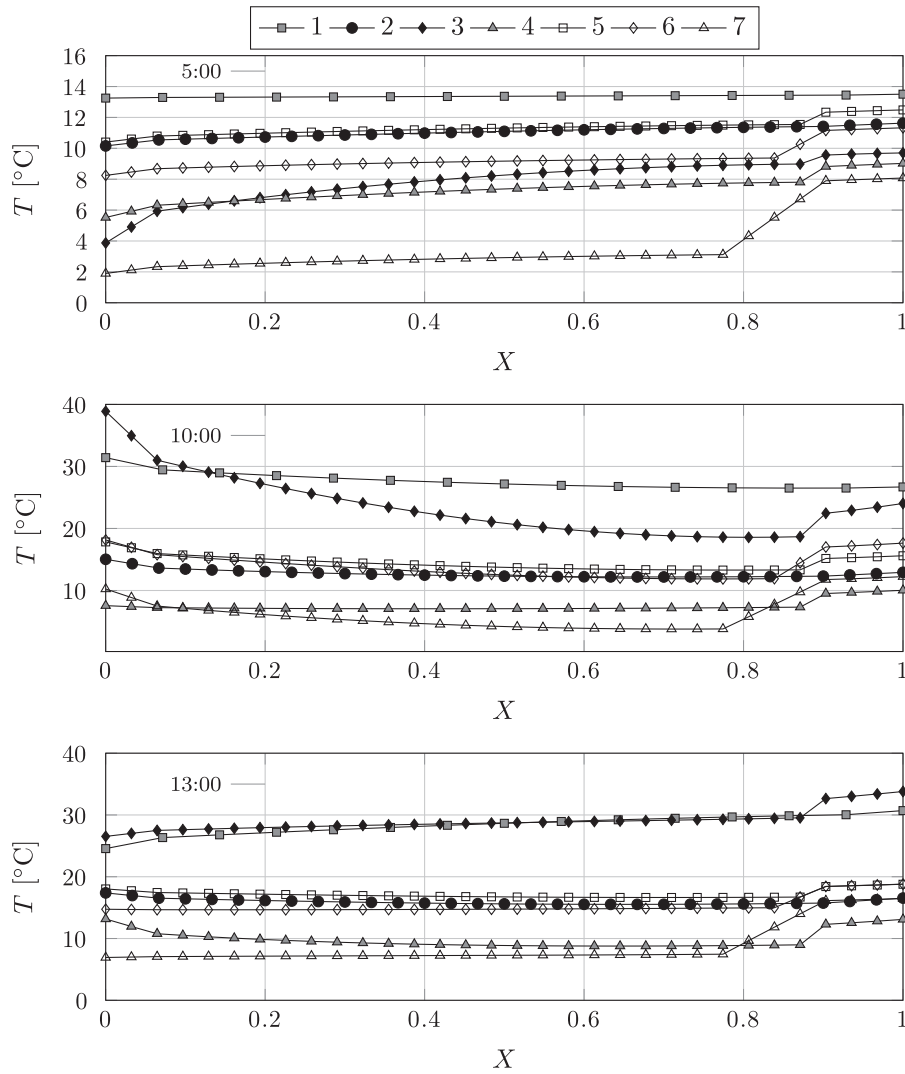
Fig. 10. Wall temperature distribution in the envelope during winter at different times.

1. In thermal zones 2–6, especially in thermal zone 3, a temperature gradient is evident, which implies greater heat losses. In the southern thermal zone 7, the effect of thermal insulation is clearest, showing a linear temperature distribution. At 10:00 h, the temperature distribution is almost constant in thermal zones 1 and 6. In thermal zones 2, 3 and 5 the outer temperature becomes higher than the inner temperature. Therefore, there is a higher heat flow across the envelope of the dwellings located in these zones. In thermal zones 6 and 7 the inner and outer temperatures are quite similar, and the presence of an insulation layer is noticeable in the latter case. In the afternoon, the temperature distributions become nearly constant in thermal zones 1–5. In the distributions corresponding to thermal zones 2 and 3 it is seen that the temperature in the envelope is higher than the outer and inner temperatures, which is evidence that there was heat accumulation in the envelope during midday.

In an *autumn* day (04/19), the temperature distribution along the thermal envelope is shown in Fig. 9. At 5:00 h the effect of the insulation layer in thermal zones 5, 6 and 7 is seen. The temperature distribution is quite similar along the envelope in thermal zones 1 and 2, while in thermal zones 3 and 4 there is a higher temperature gradient, therefore greater heat losses from the dwellings to the environment. Later (10:00 h), it is seen that the outer temperature becomes higher in thermal zones 1 and 3, increasing the inner temperature of the dwellings. The effect of the insulation

layer was effective earlier, and it is fairly noticeable in thermal zone 3. In thermal zones 2 and 4 the temperature distribution is almost constant, while in thermal zones 5, 6 and 7 the inner temperature is higher than the outer temperature and the effect of the insulation layer is still evident. In the afternoon (13:00 h), in thermal zones 1, 2 and 3 the inner temperature is higher than the outer temperature. During the morning the thermal envelope has accumulated heat, then the envelope released this stored heat to the inside of the dwelling. The temperature distribution in the envelope of the dwellings in thermal zones 4 and 5 are quite similar. The temperature in the envelope is lower than the inner and outer temperatures. This is an expected outcome after the heat stored during the morning is released from the envelope to the outer and inner environments. In the colder thermal zones 6 and 7 the inner temperature is still higher than the outer temperature and the effect of the insulation layer is noticeable.

Fig. 10 shows the temperature distribution for a *winter* day (07/19). At 5:00 h the temperature distribution is practically constant in thermal zones 1 and 2. In the other zones the temperature distribution shows the effect of the insulation layer, especially in thermal zone 7. Later, at 10:00 h the outer temperature becomes higher in thermal zones 1–5. This is more evident in thermal zone 3. In thermal zone 6 the temperature distribution is almost constant at a value close to a comfort temperature, while in thermal zone 7 the effect of the insulation layer is noticed and the inner
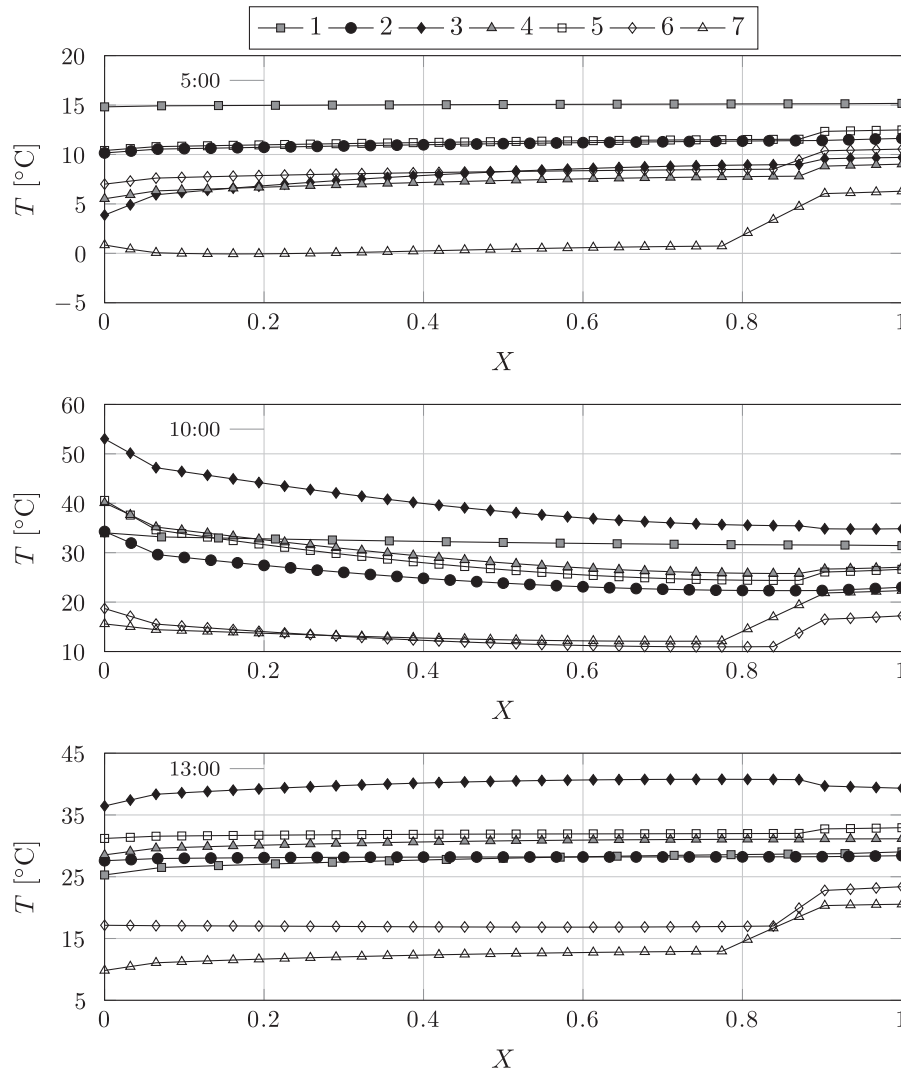
Fig. 11. Wall temperature distribution in the envelope during spring at different times.

Table 6

Outer temperature (°C) in each thermal zone at three different times (h) in chosen summer (01/18), autumn (04/19), winter (07/19) and spring (10/18) days.

Zone	Season											
	Summer			Autumn			Winter			Spring		
	t(h) = 5	10	13	5	10	13	5	10	13	5	10	13
1	14.7	21.2	21.2	**14.0**	19.2	19.9	**13.8**	14.9	15.9	14.9	17.8	18.8
2	15.5	19.7	25.2	**17.0**	17.3	18.0	10.4	11.6	12.4	11.2	15.2	16.4
3	11.6	23.1	28.2	7.1	10.5	18.1	−0.6	7.0	16.3	5.9	18.2	23.8
4	10.5	21.9	16.7	13.4	15.7	17.6	5.5	7.9	10.3	4.5	12.4	12.8
5	12.2	17.8	23.9	**13.8**	15.0	15.7	10.1	11.9	13.2	3.5	12.0	17.1
6	11.0	13.8	18.5	12.0	15.7	13.0	8.4	9.2	11.4	7.5	7.9	9.5
7	7.3	10.5	12.9	7.1	8.7	10.5	2.0	2.5	4.6	−1.5	4.3	4.7

Bold number values are higher than the inner temperature.

temperature is also close to a comfort temperature. After midday (13:00 h) and in comparison to the previous time, the inner temperatures decrease in thermal zones 1–5, and the temperature distributions become almost constant. In thermal zones 6 and 7 the comfort thermal conditions are still achieved at this time.

During the chosen *spring* day (10/18), the temperature distribution along the thickness of the envelope are shown in Fig. 11. At 5:00 h it is seen that the temperature distribution is nearly constant in 1, 2 and 5, while, in thermal zones 3, 4, 6 and 7 the inner temperature is higher than the outer temperature and the effect of the insulation layer is more noticeable in thermal zone

7. Later in the morning (10:00 h), the inner temperatures becomes lower than the outer temperatures in thermal zones 1–5. During the colder hours of the morning the dwellings in these zones loose heat though the envelope. In thermal zones 6 and 7 the effect of the insulation layer in preventing heat losses from the inside of the dwellings can be noticed. After midday (13:00 h), nearly constant temperatures are found in thermal zones 1, 2, 4 and 5. In thermal zone 3 it can be seen that the temperature in the envelope is higher than the inner and outer temperatures. This is explained by the heat accumulation that took place in the envelope during midday. Again, the effect of the insulation layer can be noticed in the colder

Table 7
Temperature (°C) of the living-room of the dwelling in each thermal zone at three different times (h) in chosen summer (01/18), autumn (04/19), winter (07/19) and spring (10/18) days.

Zone	Season											
	Summer			Autumn			Winter			Spring		
	t(h) = 5	10	13	5	10	13	5	10	13	5	10	13
1	15.4	38.3	31.3	13.1	36.3	36.1	13.9	26.5	33.3	15.4	29.6	29.5
2	17.1	30.4	33.0	16.0	**18.2**	**20.7**	12.1	14.1	**17.9**	13.4	**23.7**	27.5
3	18.0	34.3	37.7	15.0	30.4	36.3	9.7	27.2	35.3	14.0	34.0	37.4
4	16.3	29.8	28.1	16.8	**18.9**	25.9	9.4	11.0	14.5	10.4	27.0	29.8
5	17.1	**25.2**	32.2	13.9	16.4	17.4	12.8	16.4	**19.1**	10.9	27.0	32.0
6	15.6	18.5	**23.9**	12.9	**19.5**	**18.1**	11.7	**18.6**	**18.9**	10.8	18.0	**23.4**
7	12.0	17.6	21.7	11.1	**17.6**	**18.6**	8.4	13.0	16.4	6.6	**22.0**	**19.8**

Bold number values are in the comfortable temperature range.

Table 8
Variation of the measured thermophysical properties of the light building materials studied in the temperature range from −5 °C to 40 °C.

Thermal property	Fiber cement board	Polystyrene foam	Plasterboard
k (%)	10.54	16.24	6.81
α (%)	3.93	16.24	6.28

thermal zones 6 and 7, and comfort thermal conditions are achieved at this time.

7. Conclusions

The thermal properties of thermal conductivity and heat capacity were experimentally measured for some light building materials commonly used in the construction of dwellings in Chile. The properties were measured in the temperature range from −5 °C to 40 °C by the transient line heat source method. Table 8 shows the percentage variation of the measured thermal properties in the temperature range and the larger shifts are found for polystyrene foam.

The measured properties were implemented in the transient simulation of the thermal performance of a social dwelling located in each of the thermal zones of Chile. The analysis was performed during a whole year for the temperature profile in a wall of the envelope and the temperature of the living-room. According to the results, thermal comfort conditions are more likely to found in thermal zones 6 and 7 located in the south of Chile. In the northern zones (1 and 2), the predicted temperatures are very high and the effect of the insulation layer on the temperature distribution of the envelope is not important. By the contrary, the effect of the thermal insulation layer in the temperature distribution of the envelope of the dwellings located in southern Chile is more important, especially during the colder seasons. Despite the fact that numerical results were no experimentally validated, the obtained results for the dwellings located in the south of Chile are considered a good approximation to the actual thermal behavior, since according to the Chilean regulation, an appropriate thermal envelope would maintain comfort conditions in absence of internal loads. Nevertheless, it was not the case in northern locations. Therefore, in a future work a field study of the thermal performance of social dwellings located in the northern region of Chile will be performed.

Acknowledgements

References

[1] L. Pérez-Lombard, J. Ortiz, C. Pout, A review on buildings energy consumption information, Energy Build. 40 (3) (2008) 394–398, http://dx.doi.org/10.1016/j.enbuild.2007.03.007. http://www.sciencedirect.com/science/article/pii/S0378778807001016 .

[2] A. Boyano, P. Hernandez, O. Wolf, Energy demands and potential savings in european office buildings: case studies based on energyplus simulations, Energy Build. 65 (2013) 19–28, http://dx.doi.org/10.1016/j.enbuild.2013.05.039. http://www.sciencedirect.com/science/article/pii/S0378778813003277 .

[3] Z. O'Neill, X. Pang, M. Shashanka, P. Haves, T. Bailey, Model-based real-time whole building energy performance monitoring and diagnostics, J. Build. Perform. Simul. 7 (2) (2014) 83–99, http://dx.doi.org/10.1080/19401493.2013.777118, arXiv:http://dx.doi.org/10.1080/19401493.2013.777118 http://dx.doi.org/10.1080/19401493.2013.777118 .

[4] P. Hoes, J. Hensen, The potential of lightweight low-energy houses with hybrid adaptable thermal storage: comparing the performance of promising concepts, Energy Build. 110 (2016) 79–93, http://dx.doi.org/10.1016/j.enbuild.2015.10.036. http://www.sciencedirect.com/science/article/pii/S0378778815303509 .

[5] C.A. Agostini, M.C. Plottier, E.H. Saavedra, La demanda residencial de energía eléctrica en chile, Econ. Chilena 15 (3) (2012) 64–83. http://www.bcentral.cl/es/faces/bcentral/investigacion/revistaeconomia/revistas/ficharevista?id=BCCH_PUBLICACI_103707_ES&_afrLoop=79311168706034&_afrWindowMode=0&_afrWindowId=7q7ay6ad0_345#%40%3F_afrWindowId%3D7q7ay6ad0_345%26_afrLoop%3D79311168706034%26id%3DBCCH_PUBLICACI_103707_ES%26_afrWindowMode%3D0%26_adf.ctrl-state%3D7q7ay6ad0_393 .

[6] Estudio de usos finales y curva de oferta de la conservación de la energía en el sector residencial, Cámara chilena de la construcción, 2010. <http://antiguo.minenergia.cl/minwww/export/sites/default/05_Public_Estudios/descargas/estudiosUsos_Finales_COC_Sector_Residencial_2010.pdf>.

[7] F. Aldawi, F. Alam, I. Khan, M. Alghamdi, Effect of climates and building materials on house wall thermal performance, Proc. Eng. 56 (2013) 661–666, http://dx.doi.org/10.1016/j.proeng.2013.03.175, 5th {BSME} International Conference on Thermal Engineering http://www.sciencedirect.com/science/article/pii/S1877705813005298 .

[8] E. Rodriguez-Ubinas, S. Rodriguez, K. Voss, M.S. Todorovic, Energy efficiency evaluation of zero energy houses, Energy Build. 83 (2014) 23–35, http://dx.doi.org/10.1016/j.enbuild.2014.06.019, {SCIENCE} {BEHIND} {AND} {BEYOND} {THE} {SOLAR} {DECATHLON} {EUROPE} 2012 http://www.sciencedirect.com/science/article/pii/S0378778814005015 .

[9] L. Long, H. Ye, Effects of thermophysical properties of wall materials on energy performance in an active building, Energy Proc. 75 (2015) 1850–1855, http://dx.doi.org/10.1016/j.egypro.2015.07.161, Clean, Efficient and Affordable Energy for a Sustainable Future: The 7th International Conference on Applied Energy (ICAE2015) http://www.sciencedirect.com/science/article/pii/S1876610215009297 .

[10] F. Goia, B. Time, A. Gustavsen, Impact of opaque building envelope configuration on the heating and cooling energy need of a single family house in cold climates, Energy Proc. 78 (2015) 2626–2631, http://dx.doi.org/10.1016/j.egypro.2015.11.328, 6th International Building Physics Conference, {IBPC} 2015 http://www.sciencedirect.com/science/article/pii/S1876610215020603 .

[11] J.D. Spitler, D.E. Fisher, C.O. Pedersen, The radiant times series cooling load calculation procedure, ASHRAE Trans. 103 (1) (1997) 503–518.

[12] P. Loutzenhiser, H. Manz, C. Felsmann, P. Strachan, G. Maxwell, An empirical validation of modeling solar gain through a glazing unit with external and internal shading screens, Appl. Therm. Eng. 27 (23) (2007) 528–538, http://dx.doi.org/10.1016/j.applthermaleng.2006.06.016. http://www.sciencedirect.com/science/article/pii/S135943110600233X .

[13] P.C. Tabares-Velasco, C. Christensen, M. Bianchi, Verification and validation of energyplus phase change material model for opaque wall assemblies, Build. Environ. 54 (2012) 186–196, http://dx.doi.org/10.1016/j.buildenv.2012.02.019. http://www.sciencedirect.com/science/article/pii/S0360132312000583 .

[14] R.J. Howlett, W. Pereira, A. Bgl, T. Natschlger, seb-14 sensitivity analysis and validation of an energyplus model of a house in upper austria, Energy Proc. 62 (2014) 472–481, http://dx.doi.org/10.1016/j.egypro.2014.12.409. http://www.sciencedirect.com/science/article/pii/S1876610214034407 .

[15] A.S. Anelkovi, I. Mujan, S. Daki, Experimental validation of a energyplus model: application of a multi-storey naturally ventilated double skin faade, Energy Build. 118 (2016) 27–36, http://dx.doi.org/10.1016/j.enbuild.2016.02.045. http://www.sciencedirect.com/science/article/pii/S0378778816301037 .

[16] C. Yan, S. Wang, K. Shan, Y. Lu, A simplified analytical model to evaluate the impact of radiant heat on building cooling load, Appl. Therm. Eng. 77 (2015) 30–41, http://dx.doi.org/10.1016/j.applthermaleng.2014.12.017. http://www.sciencedirect.com/science/article/pii/S1359431114011351 .

[17] F.R. Mazarrn, J. Cid-Falceto, I. Caas, An assessment of using ground thermal inertia as passive thermal technique in the wine industry around the world, Appl. Therm. Eng. 33–34 (2012) 54–61, http://dx.doi.org/10.1016/j.applthermaleng.2011.09.010. http://www.sciencedirect.com/science/article/pii/S135943111100490X .

[18] A. Chan, T. Chow, Energy and economic performance of green roof system under future climatic conditions in hong kong, Energy Build. 64 (2013) 182–198, http://dx.doi.org/10.1016/j.enbuild.2013.05.015. http://www.sciencedirect.com/science/article/pii/S0378778813002910 .

[19] S. Obyn, G. van Moeseke, Variability and impact of internal surfaces convective heat transfer coefficients in the thermal evaluation of office buildings, Appl. Therm. Eng. 87 (2015) 258–272, http://dx.doi.org/10.1016/j.applthermaleng.2015.05.030. http://www.sciencedirect.com/science/article/pii/S1359431115004755 .

[20] X. Nan, M. Abeysekera, J. Wu, Modelling of energy demand in a modern domestic dwelling, Energy Proc. 75 (2015) 1803–1808, http://dx.doi.org/10.1016/j.egypro.2015.07.148, Clean, Efficient and Affordable Energy for a Sustainable Future: The 7th International Conference on Applied Energy (ICAE2015) http://www.sciencedirect.com/science/article/pii/S1876610215009169 .

[21] R. Derbal, D. Defer, A. Chauchois, E. Antczak, A simple method for building materials thermophysical properties estimation, Construct. Build. Mater. 63 (2014) 197–205, http://dx.doi.org/10.1016/j.conbuildmat.2014.04.076. http://www.sciencedirect.com/science/article/pii/S0950061814003936 .

[22] N/A, American Society of Heating, Refrigerating and Air-Conditioning Engineers, Inc., 2013. <http://app.knovel.com/hotlink/toc/id:kpASHRAEC1/ashrae-handbook-fundamentals/ashrae-handbook-fundamentals>.

[23] F. Incropera, Fundamentals of Heat and Mass Transfer, Fundamentals of Heat and Mass Transfer, vol. 1, John Wiley, 2007. https://books.google.ca/books?id=_P9QAAAAMAAJ .

[24] N. Fumo, P. Mago, R. Luck, Methodology to estimate building energy consumption using energyplus benchmark models, Energy Build. 42 (12) (2010) 2331–2337, http://dx.doi.org/10.1016/j.enbuild.2010.07.027. http://www.sciencedirect.com/science/article/pii/S0378778810002574 .

[25] A.P. Gomes, H.A. de Souza, A. Tribess, Impact of thermal bridging on the performance of buildings using light steel framing in brazil, Appl. Therm. Eng. 52 (1) (2013) 84–89, http://dx.doi.org/10.1016/j.applthermaleng.2012.11.015. http://www.sciencedirect.com/science/article/pii/S1359431112007284 .

[26] M. Yazdanian, J. Klems, Measurement of the exterior convective film coefficient for windows in low-rise buildings, ASHRAE Trans. 100 (1) (1994) 1087–1096.

[27] U.S. Department of Energy, EnergyPlus Engineering Reference, eighth ed., 2016.

[28] M. Mirsadeghi, D. Cstola, B. Blocken, J. Hensen, Review of external convective heat transfer coefficient models in building energy simulation programs: implementation and uncertainty, Appl. Therm. Eng. 56 (1–2) (2013) 134–151, http://dx.doi.org/10.1016/j.applthermaleng.2013.03.003. http://www.sciencedirect.com/science/article/pii/S1359431113001543 .